[14] N. Vojnovic, M. Mitrovic, and B. Jokanovic, "Modeling of tunneling effects in epsilon-near-zero waveguide," *Microw. Rev.*, vol. 18, pp 21–27, 2012.
[15] A. Oliner, "The impedance properties of narrow radiating slots in the broad face of rectangular waveguide: Part II—Comparison with measurement," *IRE Trans. Antennas Propag.*, vol. 5, no. 1, pp. 12–20, Jan. 1957.

A Simple Model for Average Reradiation Patterns of Single Trees Based on Weighted Regression at 60 GHz

Nuno R. Leonor, Rafael F. S. Caldeirinha, Telmo R. Fernandes, and Manuel García Sánchez

***Abstract*—Due to their complex and inhomogeneous characteristics, the propagation and radiation parameters of trees and vegetation areas are very difficult and time consuming to obtain. This communication proposes a statistical method, using robust weighted local regression, to minimize the influence of the effect of the tree inhomogeneity on its reradiation pattern, allowing the evaluation of averaged reradiation functions from simple measurements. The proposed method was successfully applied to six tree specimens of both conifer and ficus species, at 60 GHz. Furthermore, once this empirical averaged function is obtained, first-order statistics can be applied to generate several simple reradiation functions, statistically identical to those obtained from measurements. Thus, allowing the full characterization of the tree under study.**

***Index Terms*—Millimeter wave radio propagation, modeling, propagation measurements, scattering, vegetation.**

I. Introduction

The presence of trees and vegetation areas in the radio path are very likely to severely affect the performance of radiowave communications, causing signal attenuation (absorption), scattering, and/or depolarization [1], [2].

Despite a plethora of propagation models available in the literature, one of the main issues while using or developing a vegetation model is the extraction of their input parameters. Empirical and semiempirical models [3]–[5] often use simple exponential equations with a very narrow set of input parameters. Notwithstanding, the accuracy of each one of these models is limited for scenarios outside the model scope [6]. Theoretical models that make use of radiowave theory to evaluate the total scattered field [7]–[10] are able to provide much more reliable signal predictions. However, the required detailed physical description of the trees present in the simulation path, e.g., leaf density, occupied canopy area, thickness and orientation [11], may become cumbersome for larger vegetation areas.

On the other hand, radiative energy transfer (RET)-based models [12]–[14] and a similar approach based on ray-tracing algorithms presented in [15], allow, to a certain degree, the detailed description of the simulation scenario. This includes the tree distribution and make use of the prior knowledge of the reradiation function of the trees under simulation, in order to define a set of input parameters required for the model engine.

Nonetheless, due to the characteristic inhomogeneity of trees, their reradiation function is dependent on the particular orientation of the tree around its vertical axis with respect to the transmitter. Thus, in order to obtain reliable reradiation measurement results, the scattered field around the tree should be recorded for several incidence angles to mitigate the tree orientation dependency, which in turns, can be rather prohibitive. For that purpose, an empirical method to minimize the influence of the specific tree specimen used for the reradiation measurements, thus simplifying the input parameter extraction of various propagation model present in the literature, is proposed.

This communication is then organized as follows. In Section II, a thorough characterization of the signal reradiation phenomena of several isolated tree specimens is presented. Section III addresses the development of a method to obtain the averaged reradiation function of a single tree from simple reradiation measurements. For that purpose, a parametric analysis on the input parameters of the robust locally weighted regression method is performed. The performance of proposed method is assessed against reradiation measurements of three conifer and three *Ficus benjamina* trees, performed in a controlled environment at 60 GHz. In Section IV, a practical application of the proposed method is presented. Finally, conclusion and directions for further work are drawn in Section V.

II. Reradiation Functions of Single Trees

A. Measurement Geometry and Procedure

Measurements intending to record the reradiation pattern of single trees, at various incidence angles, were conducted in a controlled environment. For that purpose, the geometry depicted in Fig. 1 was assembled in an anechoic chamber, where the transmitter was set at three different positions. At each receiver position, the incidence point on the tree under measurement (TUM) was kept constant, thus implying three different incidence θ angles. The receiver was set to be at 1.4 m from ground level, and it was rotated around the tree at a constant distance of 1.3 m, within an angular range from $\phi = -120^\circ$ to $\phi = 120^\circ$. Additionally, for each step of the receiver arm rotation, the TUM was rotated around its vertical axis 360° in an increment of 1°. The received signal level was recorded continuously during the tree rotation. For each tree rotation, 140 000 samples were recorded. This allows one to record several samples of the reradiation pattern of the TUM.

B. Measurement System Overview

The measurements carried out throughout this communication were performed at 60.6 GHz. For that purpose, a transmitter comprising a signal generator (SG), to provide a continuous-wave (CW) tone at 600 MHz, was used. Additionally, a 15-GHz phase-locked loop (PLL)

Manuscript received March 13, 2015; revised July 01, 2015; accepted August 24, 2015. Date of publication August 27, 2015; date of current version October 28, 2015. This work was supported in part by the Portuguese Government, Portuguese Foundation for Science and Technology, FCT, through the financial support provided under the POPH/FSE funding, in part by the Instituto de Telecomunicações, Portugal, and in part by the Spanish Ministry of Economy and Competitiveness, Project no. TEC2014-55735-C03-3R.

N. R. Leonor is with the Instituto de Telecomunicações, Leiria 2411-901, Portugal, and also with the Departmet of Teoria do Sinal e Communicacións, University of Vigo, Vigo 36200, Spain.

R. F. S. Caldeirinha and T. R. Fernandes are with the Instituto de Telecomunicações, Leiria 2411-901, Portugal, also with the School of Technology and Management, Polytechnic Institute of Leiria, Leiria 2411-901, Portugal, and also with the School of Engineering, University of South Wales, Treforest CF37 1DL, U.K. (e-mail: rafael.caldeirinha@ipleiria.pt).

M. G. Sánchez is with the Department of Teoria do Sinal e Communicacins, Universidade de Vigo, Vigo 36200, Spain.

Digital Object Identifier 10.1109/TAP.2015.2474126

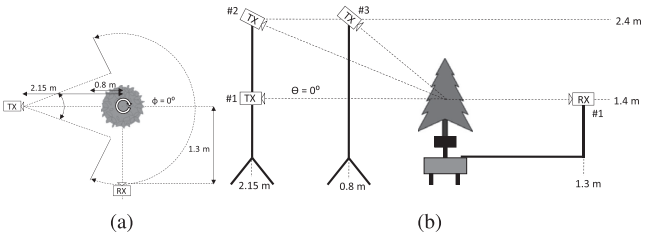

Fig. 1. Reradiation measurements inside the anechoic chamber. (a) Top view. (b) Side view.

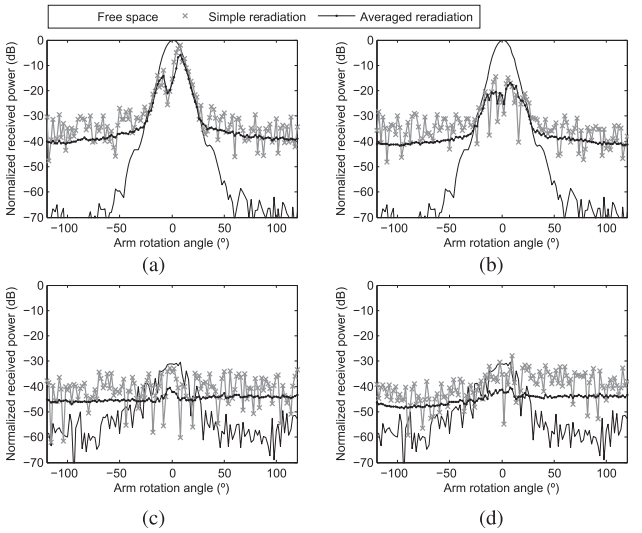

Fig. 2. 60-GHz reradiation measured results obtained for conifer tree with (a) TX#1 and (c) TX#3, and for ficus tree with (b) TX#1 and (d) TX#3.

and a frequency multiplier $(\times 4)$ were assembled, generating a 60-GHz signal carrier. The modulated radiowave was transmitted to the radio channel by a 25-dBi standard horn antenna with a half-power beamwidth of 9°.

The receiver employed a 25-dBi horn antenna, similar to that of the transmitter, coupled to a frequency mixer, for down-conversion of the received signal to a 6.6-GHz intermediate frequency (IF) signal. In this stage, a 6-GHz high-pass filter (HPF) was used to remove the lower sideband (LSB) of the received signal, thus minimizing baseband conversion interference. Finally, the 600-MHz signal was recovered through a second down-conversion, which was amplified by a 45-dB low-noise amplifier (LNA) and acquired by a spectrum analyzer (SA) remotely controlled by a GPIB interface. Simultaneously, the IF signal was also fed to a logarithmic amplifier (LogAmp), subsequently connected to a data acquisition card (DAC). To protect this measurement system, attenuators were included in both transmitter and receiver for proper adjustment of the signal levels, providing an overall system dynamic range of about 100 dB, when using the SA and about 60 dB using the DAC.

C. Measurement Results

The measurement geometry depicted in Fig. 1 was used to record the reradiation pattern of three conifer and three *Ficus benjamina* trees, for three different transmitter positions, at 60 GHz. Fig. 2 depicts an example of the recorded data, obtained from conifer tree #1 with the transmitter in positions #1 and #3, (a) and (c), respectively, as well as the measurement results obtained for ficus tree #1 with the transmitter

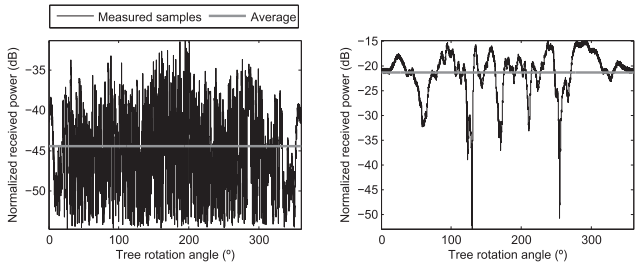

Fig. 3. Measured samples recorded during conifer tree #1 rotation with the transmitter in position #1, for (a) RX angle = $-120°$ and (b) RX angle = 0°.

in position #1 in (b) and position #3 in (d). This datum includes the free space measurement, a reradiation measurement for a constant incidence angle (gray line), and an average of all samples recorded during the tree rotation, for each receiver arm position (black dotted line). These measurement approaches and results will be often referred throughout the communication to as simple reradiation and averaged measurement, respectively.

From these measurement results, it is noteworthy that the trees will not only cause insertion loss in the forward lobe but also contribute to an increased signal level in the backscattering region. This is in line with the previous findings presented in [1] and [2]. Additionally, as one may observe in Fig. 2, as the incidence angle θ increases, i.e., at higher transmitter positions, the relationship between the front-lobe and the isotropic backscattering level is decreased. This is due to the fact that the direct coherent component is highly discriminated by the patterns of transmitter and receiver antennas, so the isotropic diffuse scattering components become more pronounced.

In order to analyze the signal variations recorded while the TUM was rotating around its vertical axis, measured samples were recorded during the rotation of conifer tree #1, for transmitter position #1, as presented in Fig. 3, for receiver arm angles of $-120°$ and 0°, (a) and (b), respectively. Similar data and signal variations were found in measurement results obtained for other trees and transmitter positions.

One may notice that the tree orientation highly affects the received signal level, which is in line with the findings presented in [16]. This effect becomes more pronounced in the front-lobe, i.e., receiver angle 0°, where nulls of 45–50 dB were found. Previous work, as described in [1], considered the depolarization of the signal as it propagates through the tree as being the most likely process responsible for such signal fadings.

D. Analysis and Discussion of Measured Results

A thorough statistical analysis was performed for all the trees and measurements under study. It was concluded that the signal variations recorded during the tree rotation follow a normal distribution around the mean value. The cumulative distribution function (cdf) of such signal variations was estimated for several tree specimens. Fig. 4(a) and (b) presents the cdf obtained with transmitter at position #1, at receiver angles $-120°$ and 0°, respectively. Similarly, Fig. 4(c) and (d) presents the cdf obtained with transmitter at position #3.

The standard deviation (σ) was also evaluated for all TUM, in the entire angular range of the receiver arm. Fig. 5(a) and (b) presents the σ values obtained for each conifer (labeled as C#1–C#3) and *ficus* (F#1–F#3) specimen, at transmitter positions #1 and #3, respectively. Considering these results, one can state that, within an error of ± 2 dB, the σ of the signal level recorded while the TUM was rotating around its vertical axis is constant in the entire receiver angular range.

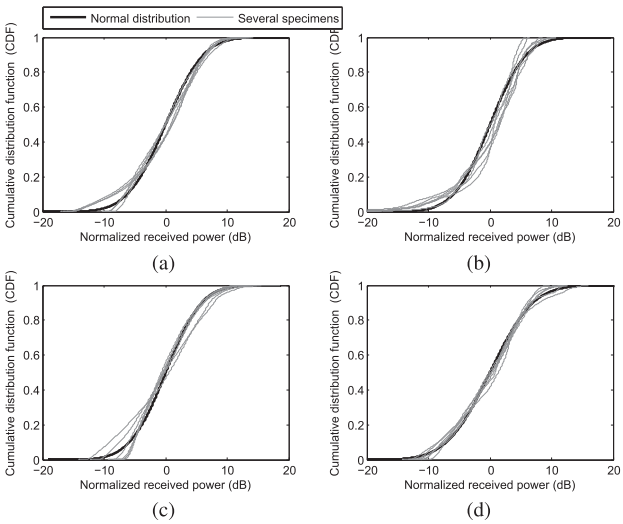

Fig. 4. CDF values for various tree specimens with TX#1, at receiver angles (a) $-120°$ and (b) $0°$, and with TX#3, at receiver angles (c) $-120°$ and (d) $0°$.

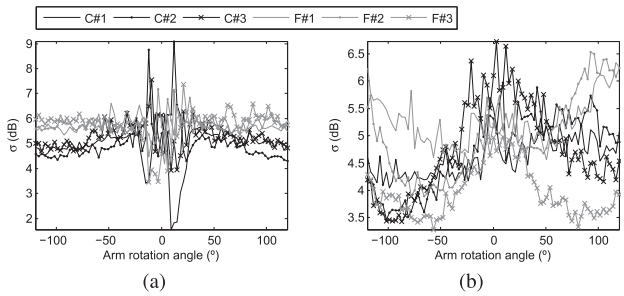

Fig. 5. σ values for various tree specimens with the transmitter in position (a) #1 and (b) #3.

III. Model Development

A. Introduction

According to [17], the reradiation pattern of a single tree is dependent on the observation (receiver) angle (ϕ), and it is expected to be described as (1), where $f(\phi)$ is a Gaussian shaped forward (main) lobe, superimposed to an isotropic level $(1-\alpha)$

$$g(\phi) = \alpha f(\phi) + (1-\alpha). \tag{1}$$

Nevertheless, the transport theory for modeling wave propagation through vegetation structures [12] relies on the assumption that the simulation volume is an homogeneous medium of uniformly distributed scatterers. This statement clashes for real forest environments where an extremely inhomogeneous media is usually found due to the irregularity of the trees, specially at signal higher frequencies. Consequently, from a simple reradiation measurement, instead of getting a smooth function as described in (1), one will find very fast and random behavior along the receiver angular range (ϕ), as observed in Fig. 2. This is due to the signal (de)polarization phenomena occurring inside the vegetation structure, and to the specific phase of each field contribution arriving at the receiver, that may randomly added or subtracted. Since the RET model does not consider the field phases as it works with "average field intensities," the reradiation function of the tree under study should be averaged.

Therefore, as originally presented in [16] for 72 samples, the experimental evaluation of $g(\phi)$ will require the measurement of the averaged reradiation function that, as described in Section II-A, includes reradiation measurements for several tree rotation angles. Thus, the experimental $\hat{g}(\phi)$ might be given by means of (2), where $x_k(\phi)$ represents several samples recorded during tree rotation for a certain receiver angle ϕ, i.e., $k = 1, \ldots, N$, with $N = 72$ in [16] and $N = 140\,000$ in the work presented herein. The experimental $\hat{g}(\phi)$ is an unbiased estimation of $g(\phi)$, and $E\left[\hat{g}(\phi)\right] \approx g(\phi)$

$$\hat{g}(\phi) = E_k\left\{x_k(\phi)\right\} = \frac{\sum_{k=1}^{N} x_k(\phi)}{N}. \tag{2}$$

According to [18], $\{x_k(t)\}$ is a nonstationary stochastic process, since its mean depends on ϕ, i.e., $\mu(\phi) = g(\phi)$, therefore, one may define it by means of (3), where $\{u(\phi)\}$ is a zero-mean stochastic process

$$y(\phi) = \{x_k(\phi)\} = g(\phi) + \{u(\phi)\}. \tag{3}$$

The mean value of a nonstationary random process $\{u(\phi)\}$ at any given ϕ might be defined by means of (4)

$$E\left[x(\phi)\right] = E\left[g(\phi) + u(\phi)\right] = E\left[g(\phi)\right] + E\left[u(\phi)\right] = g(\phi). \tag{4}$$

It follows that $g(\phi)$ can be interpreted as the instantaneous mean value of $\{x(\phi)\}$ [18]. If it is assumed that the variations of $g(\phi)$ are very slow compared to the lowest frequency in $\{u(\phi)\}$, which was proved in Fig. 2, then $g(\phi)$ can be separated from $\{x_k(\phi)\}$ by low-pass filtering operations on a single sample record $\{x_k(\phi)\}$.

One of such filtering methods available in the literature is the robust locally weighted regression [19], which will be described next.

B. Robust Locally Weighted Regression

The locally weighted regression and the particular robust version of it were first proposed by Cleveland [19]. This was intended to provide a method of smoothing scattered data, creating a trend line based on data within the immediate vicinity of a given point. The smoothing procedure presented in [19] has been designed to accommodate data compliant with (5), where g is a smooth function and ϵ_i is a random variable with 0 mean value. This equation describes the stochastic process identified in (3), where $y(x_i) = \{x_k(\phi_i)\}$, $x_i = \phi_i$, and $\epsilon(x_i) = \{u(\phi_i)\}$. Thus, the smoothing method presented in [19] is suitable to be applied to the data recorded in the measurement section. The notation presented in [19] was changed to be coherent with the previous section

$$y(x_i) = g(x_i) + \epsilon(x_i). \tag{5}$$

This method is based on a three-step procedure which, considering the original data points $[\phi_i, y(\phi_i)]$, for $i = 1, \ldots, N$, has to be applied to each ith point.

In the first step, one needs to define the weights $w_n(\phi_i)$ (6) using a window function W, for all ϕ_n, $n = 1, \ldots, N$, elements to be considered in each calculation, where h_i is the rth smallest number among $|\phi_i - \phi_j|$. This introduces the concept of span f, which manages the number of elements n to be considered at each ith polynomial regression

$$w_n(\phi_i) = W\left(\frac{\phi_n - \phi_i}{h_i}\right). \tag{6}$$

Several weight functions can be used to compute $w(\phi_i)$, once the following requirements are fulfilled:

1) $W(\phi) > 0$ for $|\phi| < 1$;
2) $W(\phi) = W(-\phi)$;
3) $W(\phi)$ is a nonincreasing function for $\phi \geq 0$;
4) $W(\phi) = 0$ for $|\phi| \geq 1$.

Nevertheless, for the purpose of this communication, the window function presented in (7), usually known as "tricube" function [19], was used

$$W(\phi) = \begin{cases} \left(1 - |\phi|^3\right)^3, & |\phi| < 1 \\ 0, & |\phi| \geq 1. \end{cases} \tag{7}$$

Finally, the first step is concluded when $\hat{B}_j(\phi_i)$, $j = 0, \ldots, d$, elements are obtained from a polynomial regression of degree d. $\hat{B}_j(\phi_i)$ are the values of B_j that minimize (8)

$$\sum_{n=1}^{N} w_n(\phi_i) \left(y_n - \beta_0 - \beta_1 \phi_n - \cdots - \beta_d \phi_n^d\right)^2. \tag{8}$$

The smoothed point at ϕ_i using locally weighted regression of degree d is $[\phi_i, \hat{y}(\phi_i)]$, where $\hat{y}(\phi_i)$ is the fitted value of the regression at ϕ_i according to (9)

$$\hat{y}(\phi_i) = \sum_{j=0}^{d} \hat{\beta}_j(\phi_i) \phi_i^j. \tag{9}$$

This step comprises the procedure defined in locally weighted regression method. Nevertheless, in the robust version, a new weight function is used so that the method is resilient to some data outliers.

For that purpose, in the second step, as presented in [19], a new set of weights δ_n (10) should be obtained using the "bisquare" weight function B, defined as (11), where $\epsilon(\phi_i)$ is the residual from the current fitted values, given by (12), and s is the median of the $|\epsilon|$

$$\delta_n = B\left(\frac{e_n}{6s}\right) \tag{10}$$

$$B(\phi) = \begin{cases} \left(1 - \phi^2\right)^2, & |\phi| < 1 \\ 0, & |\phi| \geq 1 \end{cases} \tag{11}$$

$$\epsilon(\phi_i) = y(\phi_i) - \hat{y}(\phi_i). \tag{12}$$

In the third and last step, the new $\hat{y}(\phi_i)$ fitted values should be obtained by fitting to a polynomial of order d using the weighted least squares with weight $\delta_n w_n(\phi_i)$ at (ϕ_n, y_n).

Finally, the robustness of the regression is defined by t, representing the number of times that Steps 2) and 3) are repeated.

C. Parameter Analysis

Using polynomial regression method to obtain $\hat{g}(\phi)$ from only one sample record of $x_k(\phi)$, i.e., $k = 1$, will involve a bias error that is dependent on the number of terms in the polynomial fit [18]. To this extent, a dependency analysis on the input parameters of the smoothing method presented in [19] is presented.

According to [19], four input parameters must be defined to perform the robust locally weighted regression, namely the order d of the polynomial that is locally fit to each point of the original data, the window function W used to determine the weights, the number of iterations t of the robust fitting procedure, and the span f used to determine the amount of smoothing. A detailed description on these parameters is provided in [19].

The order d of the polynomial applied to the original data, as well as the weight window function W, was defined as recommended in [19], i.e., one used $d = 1$, which should provide the adequate tradeoff between the amount of smoothing and computational effort, and the "tricube" function, whose ϕ_n elements near ϕ_i will be more important in the evaluation of the empirical $\hat{y}(\phi_i)$ than those near the span f limits.

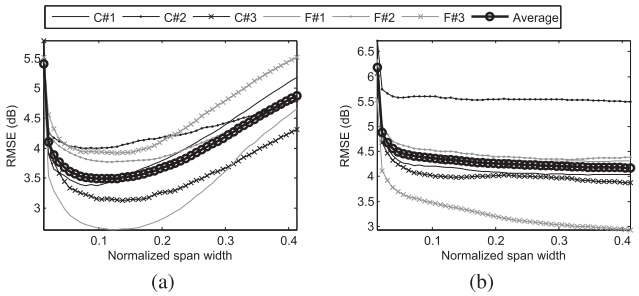

Fig. 6. Span optimization with $t = 1$ for various trees specimens and transmitter at positions (a) #1 and (b) #3.

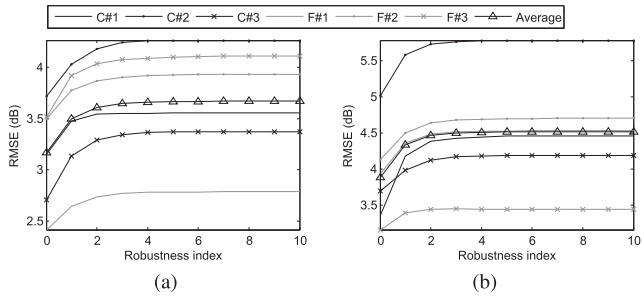

Fig. 7. Robustness optimization with $f = 0.1292$ for various trees specimens and transmitter at positions (a) #1 and (b) #3.

As far as the definition of the two remaining parameters, f and t, is concerned, an extensive parametric study was performed to assess the parameter value more suitable to evaluate averaged reradiation functions from simple measurements. In the first step, one used several simple reradiation measurements as $y(\phi_i)$, and applied the smooth method for various values of f. The resultant data, i.e., the evaluated $\hat{y}(\phi_i)$, were then compared against the respective averaged measurement. This optimization process was performed for various values of t. Fig. 6 presents the root-mean-squared-error (RMSE) dependence with f, obtained for several trees, in transmitter position #1 and #3, (a) and (b), respectively.

In the second step of the parametric analysis, the simple reradiation measurements were again used to obtain the smoothed $\hat{y}(\phi_i)$. Nevertheless, in this step, the regression method was applied for several values of t. Fig. 7 presents the RMSE variation for several values of t, obtained for all the trees under study, with the transmitter in position #1 (a) and in position #3 (b).

From this thorough parametric study, which included several measurements with an extensive range of measured samples, it was concluded that the ordered pair $(f, t) = (0.1292, 0)$, which corresponds to a span of 31 elements, is the most suitable to obtain the empirical averaged reradiation function.

D. Analysis of Model Performance

The proposed methodology to obtain the empirical averaged reradiation data from simple measurements was applied to all the experimental data obtained in Section II, which included the reradiation measurements of three conifers and three *Ficus benjamina* trees, obtained at 60 GHz for three different transmitter positions. Fig. 8 depicts the model predictions for conifer tree #1, with the transmitter in position #1 and #3, (a) and (c), respectively, as well as, for ficus tree #1, (b) and (d).

Subsequently, a quantitative assessment on the performance of the proposed method to estimate the averaged measurements from

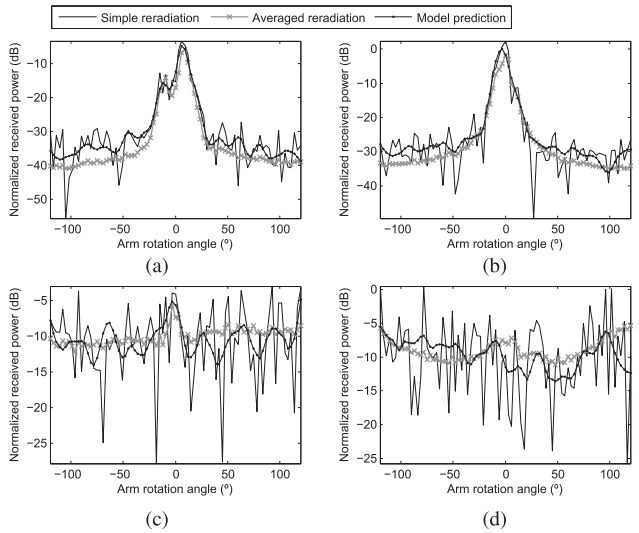

Fig. 8. Model performance obtained for conifer tree with (a) TX#1 and (c) TX#3, and for ficus tree with (b) TX#1 and (d) TX#3.

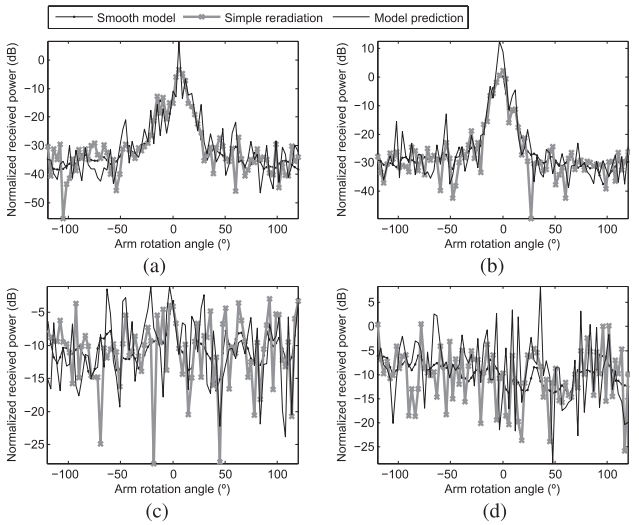

Fig. 9. Proposed model applied at results obtained for conifer tree with (a) TX#1 and (c) TX#3, and for ficus tree with (b) TX#1 and (d) TX#3.

TABLE I
RMSE OBTAINED AT 60 GHZ

TX position #	Tree #	RMSE (dB)			
		Smooth model		Simple measurements	
		Conifer	Ficus	Conifer	Ficus
1	1	3,4	2,8	5,2	5,2
	2	4,0	3,9	5,4	5,4
	3	3,3	4,0	5,8	5,5
2	1	2,4	2,8	4,6	5,2
	2	2,2	3,8	4,9	5,5
	3	3,4	3,3	5,8	5,8
3	1	1,8	2,3	5,7	5,5
	2	1,9	2,2	4,8	5,0
	3	2,1	3,4	5,3	5,6
Mean (dB)		2,7	3,2	5,3	5,4

simple reradiation data was conducted. In this analysis, one compared the averaged reradiation measurements with both model prediction and with the results obtained from simple measurements, through an RMSE analysis. Table I presents the results of this quantitative assessment.

From these results, one may conclude that the proposed method presents a relatively good estimation of the averaged measurement function, with an RMSE lower than the obtained from simple measurements. Furthermore, given its simplicity, this method will simplify the evaluation of the reradiation function of the trees, widely used as input parameter for various propagation models present in the literature.

IV. MODEL APPLICATION

A model that allows one to use simple reradiation measurements to obtain an empirical averaged reradiation function from trees was presented. This methodology will simplify the input parameter extraction for various propagation models in vegetation media, present in the literature. Additionally, the σ variation was observed to be relatively small over the entire angular range of the receiver, and thus it was assumed to be constant.

To this extent, by measuring the simple reradiation pattern of a single tree, and by evaluating the σ value for one point of the receiver rotation, one can use first-order statistics to generate several empirical simple reradiation patterns. This can be used to create a full characterization of the tree reradiation pattern, for every tree orientation angle, using a simple reradiation measurement. This can be performed using the following recipe: 1) measure an instantaneous reradiation function and the σ value for one receiver position; 2) extract the smooth model $\hat{y}(\phi_i)$ for the measured tree; and 3) create various simple reradiation functions from the smooth model plus a normal distribution, i.e., $\hat{y}_{simple}(\phi) = \mathcal{N}(\hat{y}(\phi), \sigma^2)$, where $\mathcal{N}$ stands for normal distribution.

Fig. 9 depicts an example of this model application, where the smooth model (blue line) was obtained from simple reradiation measurement (red line), and subsequently was used to generate an instantaneous reradiation function (black line), which is statistically identical to all the recorded samples during the averaged measurement. As one may observe, a relatively good convergence was obtained between measured and predicted values.

V. CONCLUSION

In this communication, a statistical model, based on weighted polynomial regression, to minimize the random component due to the tree inhomogeneity, on the trees' reradiation pattern, was proposed. This model consists in using the regression method applied to simple reradiation measurements, to obtain an empirical function which is suitable to characterize the averaged reradiation pattern of a single tree. Consequently, the burden of time-consuming process usually required to fully characterize the reradiation pattern of a single tree is thus significantly reduced. The proposed model was assessed against reradiation measurements performed in a controlled environment at 60 GHz, which included three conifer and three *Ficus benjamina* trees, and for three different transmitter positions, where a relatively good agreement between measured and predicted results was achieved.

Finally, the empirical data obtained from the regression method were successfully used to generate several simple reradiation functions, statistically identical to the measured ones, yielding RMSE errors of about 3 dB.

REFERENCES

[1] R. Caldeirinha, "Radio characterisation of single trees at micro- and millimetre wave frequencies," Ph.D dissertation, Radiowave Propag. Syst. Des. Res. Unit, Univ. Glamorgan, Pontypridd, U.K., Apr. 2001.

[2] Radiocommunication Assembly, "Recommendation ITU-R P.833–8," Attenuation in vegetation, ITU-R, 2013.
[3] M. Weissberger, "An initial critical summary of models for predicting the attenuation of radio waves by trees," Dept. Defense, Annapolisc, MD, USA, Tech. Rep. ESD-TR-81-101, 1982.
[4] Y. Meng, Y. Lee, and B. Ng, "Empirical near ground path loss modeling in a forest at VHF and UHF bands," *IEEE Trans. Antennas Propag.*, vol. 57, no. 5, pp. 1461–1468, May 2009.
[5] A. Seville and K. Craig, "Semi-empirical model for millimeter wave vegetation attenuation rates," *Electron. Lett.*, vol. 31, pp. 1507–1508, Aug. 1995.
[6] F. Wang and K. Sarabandi, "A physics-based statistical model for wave propagation through foliage," *IEEE Trans. Antennas Propag.*, vol. 55, no. 3, pp. 958–968, Mar. 2007.
[7] S. Torrico and H. Lang, "Wave attenuation prediction through a volume of random located lossy-dielectric branches 3-D vector transport theory," in *Proc. 6th Eur. Conf. Antennas Propag. (EUCAP)*, Prague, Czech Republic, Mar. 2012, pp. 3342–3345.
[8] K. Chee, S. Torrico, and T. Kurner, "Radiowave propagation prediction in vegetated residential environments," *IEEE Trans. Veh. Technol.*, vol. 62, no. 2, pp. 486–499, Feb. 2013.
[9] Y. Lin and K. Sarabandi, "A Monte Carlo coherent scattering model for forest canopies using fractal-generated trees," *IEEE Trans. Geosci. Remote Sens.*, vol. 37, no. 1, pp. 440–451, Jan. 1999.
[10] F. Wang and K. Sarabandi, "An enhanced millimeter-wave foliage propagation model," *IEEE Trans. Antennas Propag.*, vol. 53, no. 7, pp. 2138–2145, Jul. 2005.
[11] F. Wang, "Physics-based modeling of wave propagation for terrestrial and space communications," Ph.D. dissertation, Electron. Eng. Comput. Sci., Univ. Michigan, Ann Arbor, MI, USA, 2006.
[12] R. Johnson and F. Schwering, "A transport theory of millimeter wave propagation in woods and forest," Forth Monmouth, Oceanport, NJ, USA, Tech. Rep. CECOM-TR-85-1, 1985.
[13] T. Fernandes, "A discrete RET model for micro- and millimetre wave propagation through vegetation," Ph.D. dissertation, Radiowave Propag. Syst. Des. Res. Unit, Univ. Glamorgan, Pontypridd, U.K., 2007.
[14] S. Morgadinho *et al.*, "Time-variant radio channel characterization and modelling of vegetation media at millimeter-wave frequency," *IEEE Trans. Antennas Propag.*, vol. 60, no. 3, pp. 1557–1568, Mar. 2012.
[15] N. Leonor, R. Caldeirinha, T. Fernandes, D. Ferreira, and M. Sánchez, "A 2D ray-tracing based model for micro- and millimeter-wave propagation through vegetation," *IEEE Trans. Antennas Propag.*, vol. 62, no. 12, pp. 6443–6453, Dec. 2014.
[16] F. Ulaby, T. Van Deventer, J. East, T. Haddock, and M. Coluzzi, "Millimeter-wave bistatic scattering from ground and vegetation targets," *IEEE Trans. Geosci. Remote Sens.*, vol. 26, no. 3, pp. 229–243, May 1988.
[17] F. Ulaby, T. Haddock, and Y. Kuga, "Measurement and modeling of millimeter-wave scattering from tree foliage," *Radio Sci.*, vol. 25, p. 19303, May 1990.
[18] J. Bendat and A. Piersol, *Random Data: Analysis and Measurement Procedures*, 4th ed. Hoboken, NJ, USA: Wiley, 2010.
[19] W. Cleveland, "Robust locally weighted regression and smoothing scatter plots," *J. Amer. Statist. Assoc.*, vol. 74, no. 368, pp. 829–836, Dec. 1979.

Circularly Polarized Transmitarray With Sequential Rotation in Ka-Band

Luca Di Palma, Antonio Clemente, Laurent Dussopt, Ronan Sauleau, Patrick Potier, and Philippe Pouliguen

***Abstract*—We present here the design and demonstration of a circularly polarized (CP) transmitarray antenna operating in Ka-band and illuminated by a linearly polarized (LP) source. The proposed design is based on a CP unit-cell with simulated insertion loss of 0.2 dB at 30 GHz. In order to improve the axial ratio (AR) bandwidth, the sequential rotation technique is applied to the full array configuration. A model based on a hybrid in-house simulation tool is also proposed to predict accurately the array performance. The realized prototype, formed by 400 unit-cells, has 1 bit of phase resolution. The measured broadside gain is 22.8 dBi at 30 GHz with a 3-dB bandwidth of 20% in right-handed CP (RHCP). The obtained 3-dB AR bandwidth of 24.4% is comparable with higher resolution designs.**

***Index Terms*—Circular polarization (CP), discrete lens, sequential rotation, transmitarray.**

I. Introduction

Transmitarray antennas are planar multilayer structures illuminated by one or more focal sources placed at a distance F from the radiating panel (Fig. 1). The source illuminates the receiving layer, which is connected to the transmitting one using phase shifting elements. Their role is to compensate the electrical path length between the source and the array in order to collimate the incident power into a desired direction.

Beam scanning, wide bandwidth, low cost, no blockage effect, and possible reduced size are at the base of the increased interest for transmitarrays [1] and place this technology as a very attractive alternative to reflectarrays and traditional phased array antenna systems from C- to E-band [1], [2]. Transmitarrays can be used in radar systems, satellite communications, and in many applications where high gain and advanced beam-controls are needed. Circular polarization (CP) is also required in many of these applicative areas.

Several unit-cell designs based on different geometries have been proposed in the literature such as concentric square rings [3], Jerusalem crosses [4] or patches coupled through symmetric cross-shaped slots [5]. In all these cases, the transmission phase is controlled by tuning the geometrical dimensions of the unit-cell to achieve a perfect or discretized phase compensation. A CP beam can be obtained with CP sources and double linearly polarized (LP) unit-cells [4]–[6]. In this case, its polarization purity depends directly on the focal source

Manuscript received March 26, 2015; revised July 17, 2015; accepted August 18, 2015. Date of publication August 27, 2015; date of current version October 28, 2015. This work was supported by the French Ministry of Defense (Direction Générale de l'Armement).

L. Di Palma, A. Clemente, and L. Dussopt are with the CEA-LETI, F38054 Grenoble, France (e-mail: luca.dipalma@cea.fr; antonio.clemente@cea.fr; laurent.dussopt@cea.fr).

R. Sauleau is with the Institute of Electronics and Telecommunications of Rennes (IETR), UMR CNRS 6164, University of Rennes 1, F35042 Rennes, France (e-mail: ronan.sauleau@univ-rennes1.fr).

P. Potier is with the Direction Générale de l'Armement (DGA), F35174 Bruz Cedex, France (e-mail: patrick.potier@intradef.gouv.fr).

P. Pouliguen is with the Direction Générale de l'Armement (DGA), Strategy Directorate, Office for Advanced Research and Innovation, F92221 Bagneux Cedex, France (e-mail: philippe.pouliguen@intradef.gouv.fr).

Color versions of one or more of the figures in this communication are available online at http://ieeexplore.ieee.org.

Digital Object Identifier 10.1109/TAP.2015.2474149